Journal of Thermal Analysis and Calorimetry, Vol. 90 (2007) 3, 833–839

THERMAL BEHAVIOUR OF $[Mg(DMSO)_6](NO_3)_2$

A. Migdał-Mikuli and N. Górska*

Jagiellonian University, Faculty of Chemistry, Ingardena 3, 30-060 Cracow, Poland

Polymorphism and thermal decomposition of $[Mg(DMSO)_6](NO_3)_2$, where DMSO $=(CH_3)_2SO$, were studied by differential scanning calorimetry (DSC) and thermogravimetry (TG). The gaseous products of the decomposition were on-line identified by a quadruple mass spectrometer (QMS). Three phase transitions have been detected for this compound in the temperature range of 95–370 K between the following solid phases: stable KIb↔stable KIa at T_{C3}=195 K, metastable KII↔supercooled K0 at T_{C2}=230 K and stable KIa→stable K0 at T_{C1}=337 K.

Thermal decomposition of the title compound proceeds in three main stages. In the first stage, which starts just above ca. 380 K, and is continued up to ca. 540 K, the compound loses in two steps four DMSO molecules per one formula unit and undergoes into $[Mg(DMSO)_2](NO_3)_2$. The second stage starts just immediately after liberating four DMSO ligands and is connected with the decomposition of $[Mg(DMSO)_2](NO_3)_2$ and the formation of a mixture of solid anhydrous magnesium sulfate, magnesium nitrate and magnesium oxide and also a mixture of gaseous products of the DMSO and $Mg(NO_3)_2$ decomposition. The third and the last stage corresponds to the decomposition of not decomposed yet magnesium nitrate and formation of magnesium oxide, nitrogen oxides and oxygen.

Keywords: *DSC, hexadimethylsulfoxidemagnesium nitrate, phase transitions, TG/QMS, thermal decomposition*

Introduction

Crystal structure, polymorphism and mechanism of the thermal decomposition of $[Mg(DMSO)_6](NO_3)_2$, called later HMgN, are so far unknown. The phase polymorphism of the compounds of the type $[M(DMSO)_6](ClO_4)_2$, where M=Co, Cd, Mn and Zn, and also of $[Co(DMSO)_6](BF_4)_2$ and $[Al(DMSO)_6]Cl_3$ was investigated by Migdał-Mikuli *et al.* [1–6] using differential scanning calorimetry (DSC) method. $[Al(DMSO)_6]Cl_3$ has only one solid-solid phase transition at T_{C1}=245 K (on heating) [6]. The other investigated compounds characterize very rich and interesting polymorphism. Namely, both stable and metastable phases have been identified. Some of these phases are orientationally dynamically disordered crystals (ODDIC) or plastic crystals [1–5].

Up to now thermal decomposition of $[Al(DMSO)_6]Cl_3$ was studied by Migdał-Mikuli *et al.* [6]. The decomposition of the aluminium compound proceeds in four main stages. In the first stage two, and in the second stage three DMSO ligands are released. In the third stage, the last molecule of DMSO is released and aluminium chloride is created. In the fourth and last stage, Al_2O_3 and carbon are formed as a result of the reaction of $AlCl_3$ with CO, which was derived from DMSO decomposition [6]. Additionally, the thermal gravimetric analysis (TG, DTG), the simultaneous evolved gas analysis with on-line quadruple mass spectrometer (SEGA/QMS) and simultaneous differential thermal analysis (SDTA) were also performed for $[M(DMSO)_6](ClO_4)_2$ compounds, where M=Co, Mn and Zn in order to enable verification of their chemical composition and stability [3–5]. It has been shown that these compounds are stable up to temperature of ca. 380 K, whereas just above this temperature they start loosing DMSO molecules.

The general aim of these studies was to carefully examine the phase polymorphism of $[Mg(DMSO)_6](NO_3)_2$ in the temperature range of 95–380 K using DSC method and to establish the mechanism of the thermal decomposition of this compound using methods of thermal analysis (TG, DTG, QMS and DSC).

Experimental

Materials

A few grams of $[Mg(H_2O)_6](NO_3)_2$ were dissolved while being slowly heated up in dimethyl sulfoxide, called later DMSO, of high chemical purity, which was previously additionally purified by vacuum distillation at low pressure. The solution was then chilled and small, white colored crystals of hexadimethylsulfoxidemagnesium nitrate were precipitated, filtered and washed with acetone. To receive crystals of

* Author for correspondence: migdalmi@chemia.uj.edu.pl

1388–6150/$20.00

Akadémiai Kiadó, Budapest, Hungary
Springer, Dordrecht, The Netherlands

proper coordination the compound under study was re-crystallized several times from DMSO solution. The obtained crystals were then dried in a desiccator over P_2O_5 for a few days. The synthesized compound reacts immediately with water vapor from the air so it was put in a sealed vessel and stored in a desiccator over P_2O_5 as a desiccant.

Methods

Before the measurements, the composition of the investigated compound was determined on the basis of carbon and hydrogen content in the DMSO ligand and nitrogen content in the NO_3^- anions, using elementary analysis on an EURO EA 3000 instrument. Elementary analysis confirmed the proper composition of the investigated compound. The average contents of the DMSO ligands as well as the NO_3^- anions were found to be equal to the theoretical values within the error limit of ca. 0.3%.

Fourier transform Raman scattering measurements (FT-RS) were performed at room temperature with a Bio-Rad spectrometer with a resolution of 4 cm^{-1}. The incident radiation (λ=1064 nm) was from the Neodymium laser YAG Spectra-Physics.

Fourier transform far and middle-infrared absorption measurements (FT-FIR and FT-MIR) were performed using a Bio-Rad FTS60V and Bruker EQUINOX-55 spectrometers, respectively, with a resolution of 2 cm^{-1}. The FT-FIR spectrum for a powdered sample suspended in polyethylene dust was recorded. The FT-MIR spectrum was recorded for a sample suspended in Nujol and for a sample suspended in hexachlorobutadiene (HCBD) between KBr pellets.

The thermogravimetric measurements (TG/DTG) were performed using a Mettler-Toledo 851^e instrument. Two series of measurements were performed in a flow (60 mL min^{-1}) of high purity dry argon (99.999%) within temperature range of 300–840 K. The TG measurements were performed at a constant heating rate of 10 K min^{-1}. At a constant heating rate besides TG and DTG curves, the simultaneous evolved gas analysis (SEGA), with on-line quadruple mass spectrometer (QMS) using a Balzer GSD 300T instrument, were also registered. The temperature was measured by a Pt–Pt/Rh thermocouple with the accuracy of ±0.5 K.

The initial DSC measurements were made at the temperature range of 95–380 K using a Perkin-Elmer PYRIS 1 DSC calorimeter for one sample with mass of 14.13 mg (sample a). The powdered sample was placed in 30 μL aluminium vessel and was closed by compression. Another empty vessel was used for reference. The instrument was calibrated by means of the melting point of indium and melting point of water, for the high and the low temperature region, respectively. The enthalpy changes (ΔH) linked up with observed transitions were calculated by numerical integration of the DSC curves under the peaks of the anomalies. The entropy changes (ΔS) were calculated using the following formula: $\Delta S=\Delta H/T_c$.

Major DSC measurements of HMgN were performed for a sample of 11.98 mg (sample b) using a Mettler Toledo 821^e calorimeter, equipped with intracooler. The powdered sample was placed in 40 μL aluminium vessel and measured under constant flow of argon (80 mL min^{-1}) in the temperature range of 210–380 K. The third sample of 27.91 mg (sample c) was measured with the same calorimeter but in aluminium vessel containing micro-hole, at 300–840 K with a heating rate equals 10 K min^{-1}. Details of the DSC experiments are the same as described in [5, 7].

The X-ray powder diffraction (XRPD) analysis of the solid products of decomposition was made with a Seifert XRD-7 diffractometer using filtrated CuK_{α_1} radiation.

Results and discussion

In order to further identify the synthesized compound and certify its purity, the FT-RS and FT-IR spectra were performed. Figure 1 shows a comparison of Raman and infrared spectra of HMgN obtained at room temperature. The cation was considered to have octahedral symmetry with nearly freely rotating CH_3 groups of DMSO ligands. Table 1 presents a list of the bands' positions, observed in the FT-RS and FTIR spectra of the studied compound, their relative intensities and assignments denoted by comparing with the literature data for several $[M(DMSO)_6]X_2$ complexes [1–6, 8–13]. These assignments proved that both the composition and molecular structure of the investigated compound were as expected.

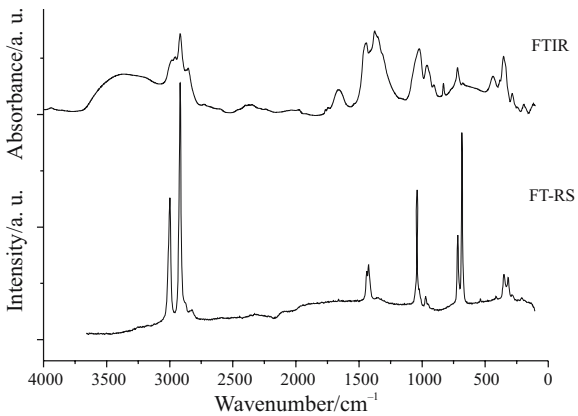

Fig. 1 Comparison of the room temperature Raman and infrared spectra of $[Mg(DMSO)_6](NO_3)_2$

Table 1 The list of bands' positions of the Raman and infrared spectra of $[Mg(DMSO)_6](NO_3)_2$ at room temperature

Frequencies/cm^{-1}					Assignments
RS		IR			
This work	DMSO [9]	This work in Nujol	This work in HCBD	DMSO [9]	
2997s	2997m	*	3008m	2985s	ν_{as}(CH)
2916vs	2913vs	*	2920m	2902s	ν_s(CH)
2824w					ν_s(CH)
1439m		*	1434s	1432s	δ_{as}(HCH)
1423m	1420m				δ_{as}(HCH)
				1401s	δ_{as}(HCH)
1355vw		*	1377vs		$\nu_3(NO_3^-)E'$
	1310w	1311m	1316m	1305m	δ_s(HCH)
1040vs					$\nu_1(NO_3^-)A_1'$
1022vw	1048vs	1020vs	1020vs	1048vs	ν_s(SO)
972w	997vw	964s	*	949m	$\rho_r(CH_3)$
	995m				$\rho_r(CH_3)$
	928vw	908m	904w		$\rho_r(CH_3)$
		831m	829m		$\nu_2(NO_3^-)A_2''$
718s		720m	713m		$\nu_4(NO_3^-)E'$
685vs	699s	681w	*	690m	ν_{as}(CS)
	670vs	617vw	*	660w	ν_s(CS)
415vw		438m	442m		ν_s(MgO)
	382m	383m		378m	δ_s(CSO)
351m	332s	355s		327m	δ_{as}(CSO)
318m	308m				δ_{as}(CSC)
289m		286m			δ_{as}(CSC)
		242w			ν_d(MgO)
212vw		197w			ν_d(MgO)
		118w			ν_L(lattice)

vw – very weak, w – weak, sh – shoulder, m – medium, s – strong, vs – very strong, br – broad;
*position of Nujol or HCBD bands

The DSC curves were obtained for each of the three HMgN samples: a, b and c at different scanning rates and at different initial and final sample heating and cooling conditions. The thermodynamic parameters of the detected phase transitions obtained from Perkin-Elmer PYRIS 1 DSC calorimeter are presented in Table 2. The results of all DSC measurements are schematically presented altogether as a temperature dependence of the free energy G (Gibbs free energy) and shown in Fig. 2.

Table 2 Thermodynamic parameters of the detected phase transitions (on heating) in $[Mg(DMSO)_6](NO_3)_2$

	T_C/K	ΔH/kJ mol^{-1}	ΔS/J mol^{-1} K^{-1}
T_{C1}	337 K±1	40.70±2.13	120.8±6.7
T_{C2}	230 K±1	7.21±0.42	31.3±1.6
T_{C3}	195 K±1	1.24±0.10	6.4±0.3

All investigated samples without any 'thermal history' are in a crystalline phase called KIa phase. The measurements on the sample a were started by cooling it from room temperature (*RT*) to 95 K, then holding it at this temperature for 1 min, and next heating it up to 300 K. The DSC curves obtained on cooling (curve 1) and subsequent heating (curve 2) of the sample a in the temperature range of 211–151 K, with a scanning rate of 30 K min^{-1}, are shown in Fig. 3. As can be seen, one small anomaly on each of these DSC curves was registered at T^h_{peak}=194.6 K (on heating) and at T^c_{peak}=191.7 K (on cooling). It is connected with the reversible stable phase transition: the KIa phase↔the KIb phase (compare with scheme in Fig. 2).

While heating sample from *RT* to 380 K with a scanning rate of 20 K min^{-1}, being initially in the KIa phase, it undergoes the phase transition at T_{C1}=337.6 K into the phase which was named the K0

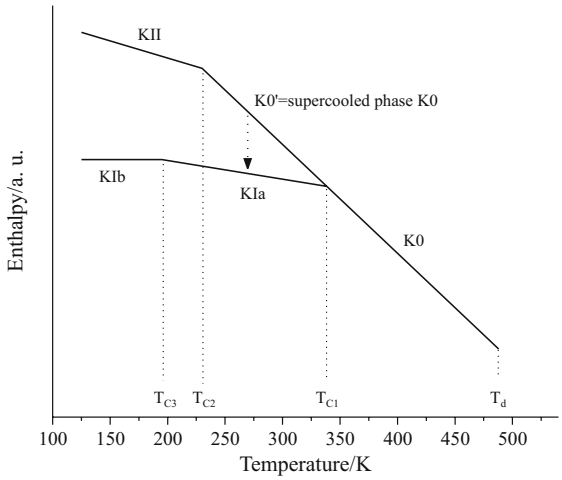

Fig. 2 Scheme of the temperature dependence of the free energy G of $[Mg(DMSO)_6](NO_3)_2$

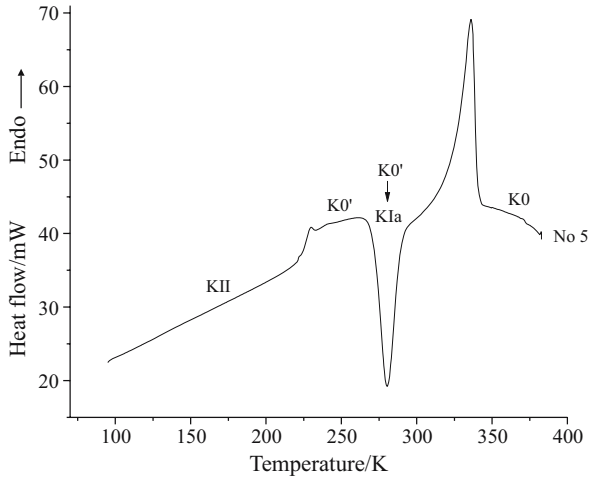

Fig. 5 DSC curve obtained in the temperature range of 95–380 K during heating of $[Mg(DMSO)_6](NO_3)_2$ with a scanning rate of 20 K min^{-1}

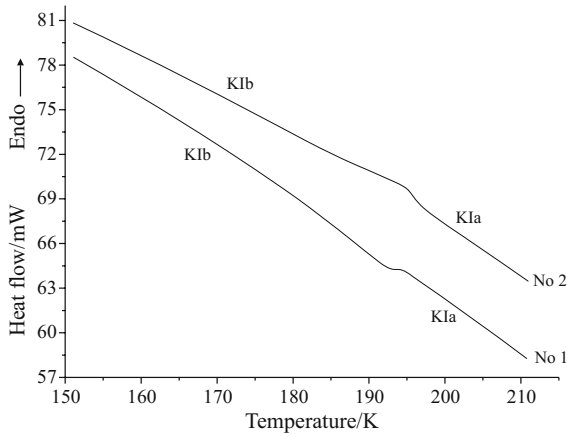

Fig. 3 DSC curves obtained during cooling (lower curve) and heating (upper curve) of $[Mg(DMSO)_6](NO_3)_2$ with a scanning rate of 30 K min^{-1} in the temperature range of 215–150 K

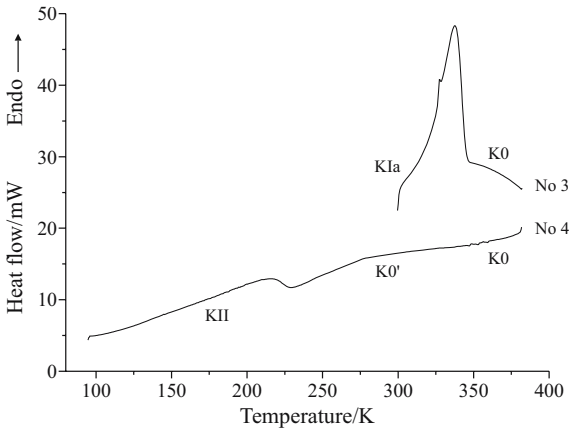

Fig. 4 DSC curves obtained during heating and cooling of $[Mg(DMSO)_6](NO_3)_2$ with a scanning rate of 20 K min^{-1}

phase. Due to this transition, a distinct anomaly on the DSC curves was recorded during heating for sample a (curve 3) and also for samples b and c. While cooling sample a, being in the K0 phase from 380 to 95 K a deep supercooling was observed. As seen in Fig. 4, there is no anomaly on the cooling curve at temperatures even much below T_{C1}. When the sample is further cooled down, a very small and broad exothermic anomaly appears at T_{C2}=230.7 K, what is connected with the transformation of the supercooled K0 phase (named K0' phase) into a metastable phase, described as the KII phase (curve 4).

The phase transition from the supercooled K0 phase to the KII phase at T_{C2} is reversible, what is clearly visible in Fig. 5. It shows the DSC curve recorded during heating (curve 5) the sample a in the temperature range of 95–380 K with a scanning rate of 20 K min^{-1}. When the sample is next heated up the KII phase transforms at T_{C2}=229.4 K into the supercooled K0 phase. Then on the DSC curve can be observed distinctive sharp exothermic peak at ca. 280 K connected with the spontaneous conversion of the supercooled K0 phase into the KIa phase. Later this stable KIa phase converts endothermically at T_{C1}=335.9 K into the stable phase K0.

The metastable nature of the supercooled K0 phase is also suggested by the DSC measurements that are given in Fig. 6. There is a distinct exothermic peak on the DSC curve 6 at ca. 268 K recorded during cooling the sample b at a rate of 5 K min^{-1}. It is connected with an exothermic process caused by relatively fast spontaneous transformation of the supercooled phase K0 to the stable KIa phase. Thus at next heating of this sample it undergoes the phase transition of the KIa phase into the stable K0 phase (curve 7).

The phase polymorphism of $[Mg(DMSO)_6](NO_3)_2$ is similar but not so rich as the polymorphism of the compounds of the type: $[M(DMSO_6](ClO_4)_2$ and $[M(DMSO_6](BF_4)_2$ studied earlier by Migdał–Mikuli *et al.* [1–5].

The thermal decomposition measurements for the compound under study were made for two samples of masses: 72.0616 and 79.0947 mg, for both at a constant heating rate of 10 K min^{-1}. Both the first and the second sample were placed in a 150 μL open corundum crucible. The results obtained for both samples are nearly identical. Figure 7 shows TG, DTG and DSC curves recorded in the temperature range of 300–840 K. During the TG experiment, the QMS spectra of masses were followed from *m*/*e*=1 to 100, however, for reasons of graphic readability, only the masses of *m*/*e*=64, 48, 78, 46, 14, 16, 44, 17, 18, 28, 15 and 30 representing SO_2, SO, CH_2SO_2 or $(CH_3)_2SO$, NO_2, CH_2 or N, CH_4 or O, N_2O or CO_2, NH_3 or OH, H_2O, N_2, CH_3 and NO, are shown in Fig. 8.

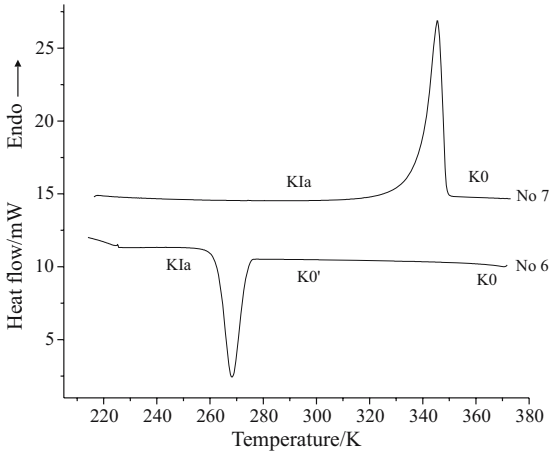

Fig. 6 DSC curves obtained in the temperature range of 215–370 K during cooling and heating of $[Mg(DMSO)_6](NO_3)_2$ with a scanning rate of 5 K min^{-1}

The TG, DTG and QMS curves show that the decomposition of the sample proceeds in three main stages (I, II, III). From the character of the TG curve obtained for this compound we can conclude that from *RT* up to temperature about 380 K the sample does not lose its initial mass. It can be observed that the first stage of decomposition, which takes place in the temperature range of 380–540 K, involves release of four DMSO ligands included in coordination sphere of magnesium atom, per one formula unit. Resulting $[Mg(DMSO)_2](NO_3)_2$ in the second stage in the temperature range of 540-610 K, immediately decomposes. Besides formation of gaseous products as: oxygen, nitrogen, water vapor, nitrogen oxides, CH_3, CH_3SO and CH_2SO_2, undergoes also the formation of magnesium compounds: $MgSO_4$, $Mg(NO_3)_2$ and MgO. The third stage in the temperature range of 610–840 K is connected with the decomposition of resulting $Mg(NO_3)_2$ to nitrogen oxides species, oxygen and solid MgO. After the third stage of the decomposition 10.6% of the initial mass of the sample remained as solid product. X-ray powder diffraction

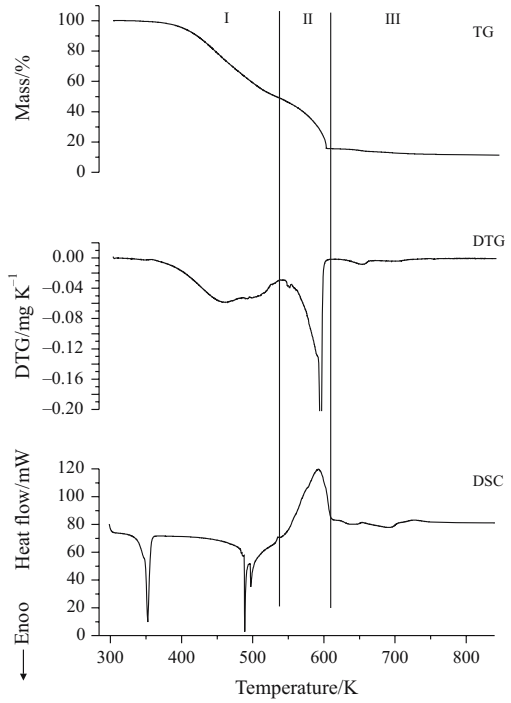

Fig. 7 TG, DTG and DSC curves for $[Mg(DMSO)_6](NO_3)_2$ in the range of 300–840 K registered at a constant heating rate of 10 K min^{-1}

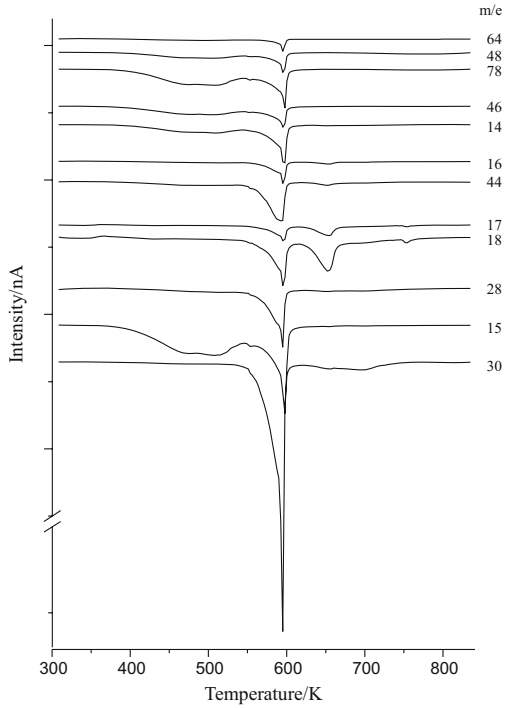

Fig. 8 QMS curves registered simultaneously with TG for $[Mg(DMSO)_6](NO_3)_2$ in the range of 300–840 K

Table 3 Parameters of $[Mg(DMSO)_6](NO_3)_2$ thermal decomposition

Sample mass/mg	Stage number	Temperature range/K	Mass loss at the stage/%	Mass after decomp./%	Mass loss $_{calc}$/%	Products of decomposition
79.0947	I ab	375–540	50.8		50.6	4 DMSO
	II	540–610	33.7		33.4	gaseous products of $[Mg(DMSO)_2](NO_3)_2$ decomposition
	III	610–840	4.9		5.1	gaseous products of $Mg(NO_3)_2$ decomposition
				10.6	10.9	$\frac{2}{3}MgO+\frac{1}{3}MgSO_4$

measurements confirmed that the solid decomposition products are anhydrous magnesium sulfate and magnesium oxide. The temperature ranges, percentage of lost mass and the products of the thermal decomposition of $[Mg(DMSO)_6](NO_3)_2$ at particular stages are presented in Table 3.

The profile of the heat flow *vs.* temperature dependence (DSC curve) for $[Mg(DMSO)_6](NO_3)_2$, when the sample is not hermetically closed, shows five endothermic peaks and one exothermic peak. The first endothermic peak occurs at about 352 K and is connected with the solid–solid phase transition of the investigated compound. The next two sharp endothermic peaks at ca. 490 and 500 K can be explained by the two steps of liberation of four DMSO ligands resulting in the formation of $[Mg(DMSO)_2](NO_3)_2$ according to the reaction (1).

At the first stage, the evolved dimethyl sulfoxide simultaneously decomposes mainly to paraformaldehyde. Dimethyl sulfide, dimethyl disulfide, *bis*(methylthio)methane and water are other volatile products. A small amount of dimethyl sulfone can also be found [14]. At higher temperatures or after the fragmentation of the above mentioned molecules, mass spectrum of DMSO contains five main groups of lines. The most intense lines in each group are situated at *m*/*z* values equal to: 15, 29, 45, 63 and 78. They may correspond to CH_3, C_2H_5, C_2H_5O, CH_3SO and CH_2SO_2, respectively [15–17].

The exothermic peak occurred in the DSC curve corresponds to the reduction and oxidation (red-ox) processes taking place between the reductants (DMSO ligands) and the oxidants (NO_3^- anions). Next two small endothermic peaks at about 640 and 690 K can be explained by the decomposition of resulting in the second stage magnesium nitrate.

The processes of thermal decomposition of $[Mg(DMSO)_6](NO_3)_2$ can be described by three main stages, but the first one has two steps:

stage Ia: $[Mg(DMSO)_6](NO_3)_2 \rightarrow [Mg(DMSO)_3](NO_3)_2+3DMSO$ (1)

stage Ib: $[Mg(DMSO)_3](NO_3)_2 \rightarrow [Mg(DMSO)_2](NO_3)_2+1DMSO.$

At the stage II resulting $[Mg(DMSO)_2](NO_3)_2$ decomposes mainly to solid magnesium nitrate, magnesium oxide and magnesium sulfate and to gaseous products of the DMSO and partial $Mg(NO_3)_2$ decomposition. Next, at stage III the rest of $Mg(NO_3)_2$ decomposes to solid magnesium oxide and to oxygen and nitrogen oxides.

The thermal decomposition of $[Mg(DMSO)_6](NO_3)_2$ in some aspects is similar and in others different to the decomposition of $[Mg(NH_3)_6](NO_3)_2$ [18] and $[Cd(NH_3)_6](NO_3)_2$ [19]. These compounds decompose also in three main stages. During the first stage $[Mg(NH_3)_2](NO_3)_2$ and $[Cd(NH_3)](NO_3)_2$ are created, respectively. However, the second stage is connected with subsequent liberation of ammonia and simultaneous reduction-oxidation processes of the part of ammonia leading to creation of the water vapor, magnesium oxide and magnesium nitrate. The last third stage concerns the decomposition of corresponding nitrates and formation of oxygen, nitrogen oxides and MgO or CdO, respectively.

Conclusions

- The following phase transitions of HMgN have been detected:
  a. reversible phase transition: stable KIb↔stable KIa at T_{C3}=195 K;
  b. reversible phase transition: metastable KII↔supercooled K0 at T_{C2}=230 K;
  c. irreversible phase transition: stable KIa→stable K0 at T_{C1}=337 K;.
- It can be concluded from the values of the entropy changes that the phase K0 and supercooled K0 must be the phases with a high degree of disorder, probably orientationally dynamically disordered crystals (ODDIC). This indicates the very big value of ΔS=120.8 J mol^{-1} K^{-1} connected with the phase transition KIa→K0 at T_{C1}. The metastable phase KII is the crystal with a high degree of rotational disorder too, but significantly less than K0 and K0' phases (big value of ΔS=31.3 J mol^{-1}K^{-1} connected with the phase transition KII→K0' at T_{C2}). The

phases KIa and KIb are more or less ordered phases (small value of ΔS=6.4 J mol^{-1} K^{-1} connected with the KIb↔KIa phase transition at T_{C3}). Phases KIa, KIb and K0 form mutually an enantiotropic system in the whole temperature range but, in a relation to the metastable KII phase, they form a monotropic system.

- The thermal decomposition of $[Mg(DMSO)_6](NO_3)_2$ proceeds in three main stages. In the first stage four molecules of DMSO are liberated. The second stage is connected with the decomposition of resulting $[Mg(DMSO)_2](NO_3)_2$ and formation of solid anhydrous $MgSO_4$, MgO, $Mg(NO_3)_2$ and other gaseous products of the DMSO and partial $Mg(NO_3)_2$ decomposition. The rest of magnesium nitrate decomposes next, in the third stage, to the oxygen, nitrogen oxides and magnesium oxide. The final products of the decomposition of the investigated compound are magnesium oxide and anhydrous magnesium sulfate.

Acknowledgements

We would like to thank E. Mikuli Ph.D., Dr.Sc. and E. Szostak Ph.D. from the Faculty of Chemistry of the Jagiellonian University for stimulating discussions. We are also grateful to M. Bućko Ph.D. from the AGH University of Science and Technology in Kraków for making the X-ray powder diffraction measurements for us.

References

1 A. Migdał-Mikuli, E. Mikuli, E. Szostak and J. Serwońska, Z. Naturforsch., 58a (2003) 341.
2 A. Migdał-Mikuli and E. Szostak, Z. Naturforsch., 60a (2005) 289.
3 A. Migdał-Mikuli and E. Szostak, Thermochim. Acta, 426 (2005) 191.
4 A. Migdał-Mikuli and E. Szostak, Thermochim. Acta, 444 (2006) 195.
5 A. Migdał-Mikuli, Ł. Skoczylas and E. Szostak, Z. Naturforsch., 61a (2006) 180.
6 A. Migdał-Mikuli, N. Górska and E. Szostak, J. Therm. Anal. Cal., OnlineFirst: DOI: 10.1007/s10973-006-7694-z.
7 A. Migdał-Mikuli, E. Mikuli, S. Wróbel and Ł. Hetmańczyk, Z. Naturforsch., 54a (1999) 590.
8 C. C. Addison and D. Sutton, J. Chem Soc., A (1966) 1524.
9 M. Sandström, I. Persson and St. Ahrland, Acta Chem. Scand., A 32 (1978) 607.
10 B. F. G. Johnson and R. A. Walton, Spectrochim. Acta, 22 (1966) 1853.
11 M. Sandström, I. Persson and St. Ahrland, Acta Chem. Scand., A 32 (1978) 607.
12 S. Ahrland and N. Björk, Acta Chem. Scand., A 28 (1974) 823.
13 D. Dembicka and A. Bartecki, Koord. Chim., 10 (1984) 1519.
14 V. J. Traynelis and W. L. Hergenrother, J. Org. Chem., 29 (1964) 221.
15 D. A. Blank, S. W. North, D. Stranges, A. G. Suits and Y. T. Lee, J. Chem. Phys., 106 (1997) 539.
16 F. C. Thyrion and G. Debecker, Intern. J. Chem. Kinet., 5 (2004) 583.
17 T. T. Lam, T. Vickery and L. Tuma, J. Therm. Anal. Cal., 85 (2006) 25.
18 A. Migdał-Mikuli, E. Mikuli, R. Dziembaj, D. Majda and Ł. Hetmańczyk, Thermochim. Acta, 419 (2004) 223.
19 E. Mikuli, M. Liszka and M. Molenda, J. Therm. Anal. Cal., OnlineFirst: DOI: 10.1007/s10973-006-7610-6.

Received: November 8, 2006
Accepted: March 9, 2007
OnlineFirst: July 5, 2007

DOI: 10.1007/s10973-006-8251-5